PCCP

PAPER

View Article Online
View Journal | View Issue

Cite this: *Phys. Chem. Chem. Phys.*, 2014, **16**, 7274

Chemical bonding in electron-deficient boron oxide clusters: core boronyl groups, dual 3c–4e hypervalent bonds, and rhombic 4c–4e bonds†

Qiang Chen, Haigang Lu, Hua-Jin Zhai* and Si-Dian Li*

Received 27th January 2014,
Accepted 20th February 2014

DOI: 10.1039/c4cp00406j

www.rsc.org/pccp

We explore the structural and bonding properties of the electron-deficient boron oxide clusters, using a series of $B_3O_n^{-/0/+}$ (n = 2–4) clusters as examples. Global-minimum structures of these boron oxide clusters are identified *via* unbiased Coalescence Kick and Basin Hopping searches, which show a remarkable size and charge-state dependence. An array of new bonding elements are revealed: core boronyl groups, dual 3c–4e hypervalent bonds (ω-bonds), and rhombic 4c–4e bonds (o-bonds). In favorable cases, oxygen can exhaust all its 2s/2p electrons to facilitate the formation of B–O bonds. The current findings should help understand the bonding nature of low-dimensional boron oxide nanomaterials and bulk boron oxides.

1. Introduction

Boron is a prototypical electron-deficient element with unique structural and bonding properties.[1] Relevant chemical species belong to the so-called "hypovalent" systems.[2] The concept of three-center two-electron (3c–2e) bonds in boranes, which effectively compensate for boron's electron-deficiency, is a cornerstone in modern chemical bonding theory.[1] Elementary boron clusters have been recently shown to be dominated by (π and σ) aromaticity and antiaromaticity, resulting in unusual planar or quasi-planar structures up to very large sizes.[3–8] Upon oxidation, boron oxide clusters[9–15] are anticipated to be even more electron-deficient, offering opportunities to explore exotic chemical bonding.

Previous combined experimental and theoretical studies have demonstrated that the boronyl (BO) group with a B≡O triple bond serves as a robust ligand in boron oxide clusters,[13–15] akin to the CN and CO/CN^- ligands, which are isovalent to BO and BO^-, respectively. However, current understanding of the chemical bonding in such systems remains limited. In this contribution, we explore the structural and bonding properties of boron oxide clusters. We choose a series of $B_3O_n^{-/0/+}$ (n = 2–4) clusters as examples. The cluster structures turn out to exhibit drastic dependence upon either the charge-state or oxygen-content. A variety of new bonding features are revealed, which we believe form the core bonding concepts in the electron-deficient boron oxide system and may be applied to other boron oxide clusters and low dimensional and bulk materials.

Nanocluster Laboratory, Institute of Molecular Science, Shanxi University, Taiyuan 030006, China. E-mail: hj.zhai@sxu.edu.cn, lisidian@sxu.edu.cn

† Electronic supplementary information (ESI) available: Natural charges, natural resonance theory bond orders and atomic valencies for the global-minimum structures of $B_3O_2^+$, $B_3O_3^{-/0/+}$, and $B_3O_4^{-/0/+}$; calculated vertical detachment energies of $B_3O_n^-$ (n = 2–4) at the TD-B3LYP level; alternative optimized structures of $B_3O_2^+$, $B_3O_3^{-/0/+}$, and $B_3O_4^{-/0/+}$; and AdNDP bonding patterns and canonical molecular orbitals of $B_3O_2^+$, $B_3O_3^{-/0/+}$, and $B_3O_4^{-/0/+}$. See DOI: 10.1039/c4cp00406j

2. Methods

Structural searches were carried out using the Coalescence Kick (CK)[16,17] and Basin Hopping (BH)[18] global-minimum search programs, initially at the B3LYP/3-21G level. Low-lying candidate structures were then fully optimized at the B3LYP/aug-cc-pVTZ level. Frequency calculations were done to confirm that the reported structures are true minima. The energetics of top structures within 20 kcal mol^{-1} was further evaluated using single-point CCSD(T) calculations[19] at the B3LYP geometries; that is, at the CCSD(T)//B3LYP/aug-cc-pVTZ level. Bonding analyses were accomplished using the canonical molecular orbitals (CMOs) and the adaptive natural density partitioning (AdNDP).[24] Natural resonance theory (NRT) bond orders were obtained from the natural bond orbital (NBO) analyses.[20] Photoelectron spectra of anion global-minimum clusters were predicted using the time-dependent B3LYP (TD-B3LYP)[21] method to facilitate their future characterizations. All calculations were done using the Gaussian 09 package.[22]

3. Results

Global-minimum structures of the $B_3O_n^{-/0/+}$ (n = 2–4) clusters are depicted in Fig. 1, which are obtained initially *via* the CK and BH structural searches and subsequently reoptimized using density-functional theory (DFT) at the B3LYP/aug-cc-pVTZ level. Low-lying structures within 20 kcal mol^{-1} are further evaluated

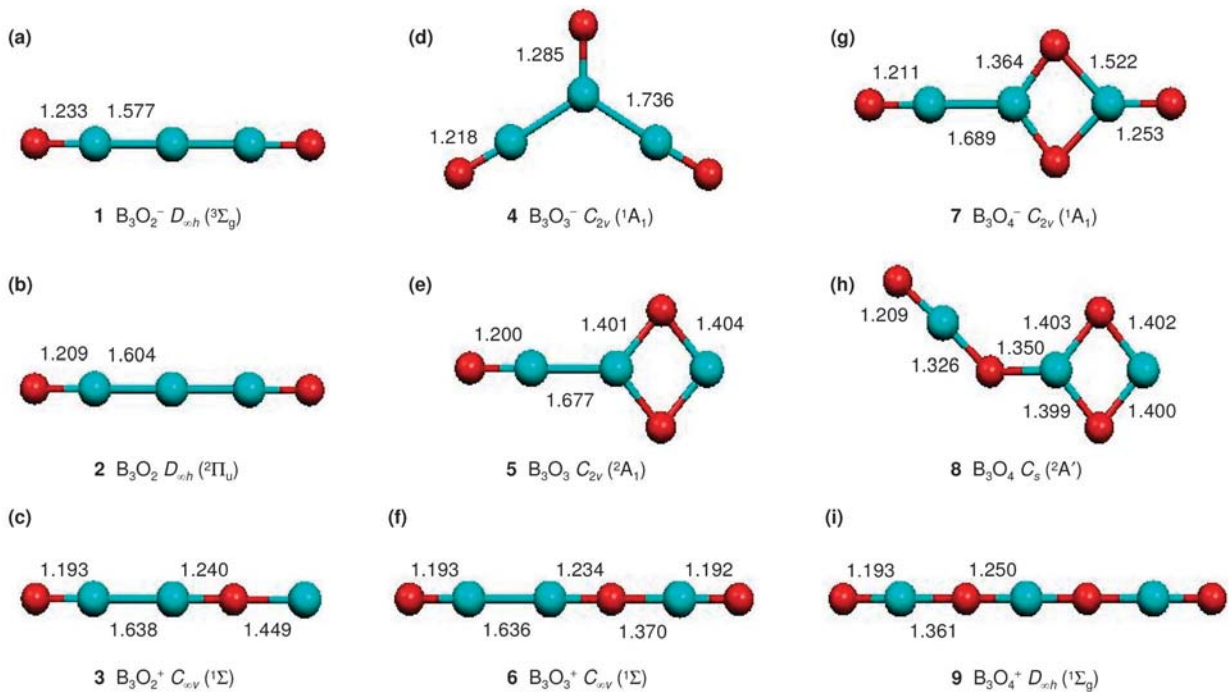

Fig. 1 Global-minimum structures **1–9** for $B_3O_n^{-/0/+}$ (n = 2–4) clusters at the B3LYP/aug-cc-pVTZ level. Bond distances (in Å) are labeled. The structures are obtained *via* the Coalescence Kick and Basin Hopping global-minimum searches.

using the single-point CCSD(T) calculations. Alternative optimized structures are collected in Fig. S1–S7 in the ESI,† except for $B_3O_2^-$ and B_3O_2 that were studied in a prior work.[13] Briefly, structures **1–6**, **8**, and **9** are at least ~10 kcal mol^{-1} lower than their alternative structures at the B3LYP and CCSD(T) levels, whereas structure **7** has two competitive isomers, being ~4 and ~6 kcal mol^{-1} higher in energy at the CCSD(T) level. In all cases, the global minima are energetically well defined.

Remarkably, for structures **1–9** (Fig. 1), every species undergoes substantial changes in atomic connectivity upon addition or removal of a charge except for the **1–2** pair, which maintain the same motif. Also, upon changing oxygen content, geometric rearrangements occur. These structural trends testify to a key idea in cluster science: every electron counts and every atom counts, making the current clusters an interesting and unique chemical system. Among the nine global-minimum clusters, five adopt linear geometries (**1–3**, **6**, and **9**) and three possess a rhombic B_2O_2 unit (**5**, **7**, and **8**).

In terms of the bond distances, the terminal BO groups (1.19–1.23 Å) in **1–9** are straightforwardly assigned to the B≡O triple bonds, that is, boronyls, which have been established lately as the structural blocks in boron oxide clusters and compounds.[9–15] The BB distances of 1.64–1.74 Å in **3–7** are assigned to single bonds.[23] The BB distances of 1.58 and 1.60 Å in **1** and **2**, with an effective bond order of 1.5 and 1.25, respectively, are slightly shorter than single bonds due to the extra three-center one-electron (3c–1e) BBB bonds.[13] The bridging BO (1.29 Å) in **4** is a typical B=O double bond. These assignments set the background for discussion below. Note that $B_3O_4^+$ was studied previously using the collision activation mass spectrum technique and a linear structure similar to **9** is proposed, albeit with markedly different bond orders.[11]

4. Discussion

4.1. Core boronyl groups

New bonding features in boron oxide clusters as revealed using $B_3O_n^{-/0/+}$ (n = 2–4) are presented in Fig. 2, which are distilled from the CMO and AdNDP[24] analyses (Fig. S8–S15 in the ESI†). AdNDP represents the electronic structure in terms of n-center two-electron (nc–2e) bonds, with the n value ranging from one to the total number of atoms in a molecule, thus recovering the classical Lewis bonding elements (lone-pairs and 2c–2e bonds), as well as the nonclassical delocalized nc–2e bonds. The CMO and AdNDP data are highly coherent with each other, allowing elucidation of the nature of bonding in the system, which are further aided by the NRT bond orders (Tables S1–S7 in the ESI†). Based on these analyses, approximate Lewis structures of **1–9** are obtained, as shown in Fig. 3.[25]

First of all, "core" boronyl groups are identified in **3** and **6** (Fig. 3), with bond distances of 1.23–1.24 Å (Fig. 1). Their identity as a B≡O triple bond is readily revealed from the CMO analyses (Fig. 2a). Here HOMO − 7 is a σ bond derived primarily from the O 2p$_x$ atomic orbital (AO), whereas HOMO − 4 and HOMO − 5 are π bonds based on O 2p$_y$ and 2p$_z$ AOs, respectively. These collectively constitute a triple bond, similar to those in the gas-phase BO, CO, and CN molecules. To our knowledge, the core boronyl group is unknown in the literature. It closely parallels the terminal and bridging boronyl groups

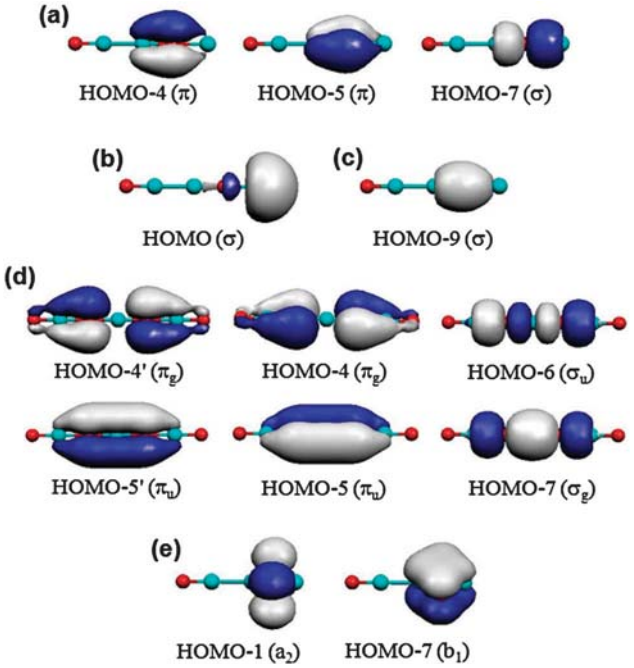

Fig. 2 Key bonding elements in the boron oxide clusters as revealed from the canonical molecular orbital analyses: (a) core B≡O triple bond in $B_3O_2^+$ (**3**); (b) terminal B with a 2s lone-pair character in $B_3O_2^+$ (**3**); (c) terminal B–O single bond in $B_3O_2^+$ (**3**), which combines with (a) to produce a formal fourfold bonded O site; (d) dual 3c–4e hypervalent π bonds (ω-bonds) in $B_3O_4^+$ (**9**); and (e) rhombic 4c–4e bonds (o-bonds) in B_3O_3 (**5**).

observed lately, which help develop the chemistry of boronyl as a new inorganic ligand.[9–15] However, differing apparently from the terminal or bridging BO group, the core boronyl group is associated with a B^+ center (Fig. 3). Consequently, B contributes only one electron to the B≡O triple bond with O contributing the remaining five, in contrast to a terminal or bridging BO group, where B and O contribute two and four electrons, respectively. Indeed, a core boronyl group appears to be more polar and ionic, with a slightly greater bond distance. For example, the core BO group in **3** possesses a NRT total bond order of 2.93 (covalent: 0.72; ionic: 2.21), as compared to 2.97 (covalent: 1.39; ionic: 1.58) for the terminal BO in the same cation (Table S1 in the ESI†).

4.2. Terminal B site with lone-pair character

A terminal B site is observed in **3** (Fig. 1c). It possesses a lone-pair with primary B 2s character (Fig. 2b). Considering that **3** is an extremely electron-deficient system, a boron lone-pair seems to be odd and counter-intuitive. A linear structure with two BB single bonds is much anticipated, but it turns out to be ~14 kcal mol^{-1} (Fig. S1 and S9 in the ESI†) above the global-minimum **3** at the single-point CCSD(T) level. A similar terminal B site was proposed previously for the $B_2O_2^+$ cation cluster.[11] We argue that the unusual global-minimum structure **3** highlights the competition between BB and BO bonding in the system, where the BO bonding appears to dominate. There are seven BO bonds and one BB bond in **3**, as compared to six BO bonds and two BB bonds in its competitor. In other words, **3** has one more BO bond in replacement of a BB bond, which explains its enhanced stability.

4.3. Dual 3c–4e hypervalent bonds

Unusual bonding situations are revealed in **3**, **6**, and **9**, including oxygen with fourfold bonds and boron with dual three-center four-electron (3c–4e) hypervalent bonds.[2] The core OBO block in **9** possesses short BO distances of 1.25 Å (Fig. 1), being close to the core boronyl groups in **3** and **6** (1.23–1.24 Å) and markedly shorter than the typical B=O double bond in **4** (1.29 Å). This observation hints that the BO bonds in the OBO core should have triple bond character, which is consistent with the self-consistent triple bond radii (r_B = 0.73 Å; r_O = 0.53 Å).[26] The corresponding CMOs are depicted in Fig. 2d. The bottom three (HOMO − 7, HOMO − 5, and HOMO − 5′) are completely bonding, composed of the overlapping of O 2p and the B 2s2p hybrid. The combination of HOMO − 6 and HOMO − 7 results in two σ bonds, constituting the OBO σ bonding in the p_x manifold.

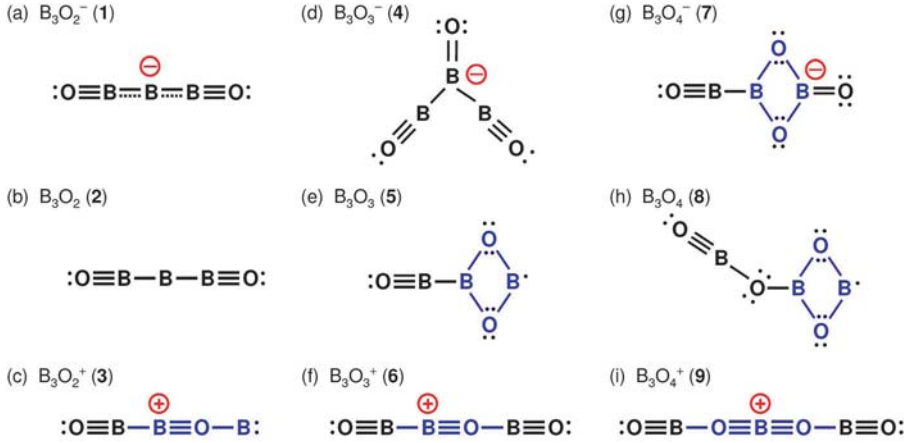

Fig. 3 Schematic Lewis presentation for the global-minimum structures **1–9** of $B_3O_n^{-/0/+}$ (n = 2–4) clusters. The three-center one-electron BBB bond in **2** is not labeled. The extra charge in an anion or a cation species is shown in red.

Formally antibonding between two BO subunits, HOMO − 4 and HOMO − 4′, is essentially nonbonding with 48% O $2p_y/2p_z$ on each O center. The *bonding*/*nonbonding* combination of HOMO − 4 and HOMO − 5 forms a 3c–4e π bond, which is reminiscent of the 3c–4e hypervalent bond (the so-called ω-bond),[2] being responsible for the three-center OBO π interaction in the p_y manifold. Similarly, HOMO − 4′ and HOMO − 5′ combine to form a 3c–4e π bond in the p_z manifold. In short, the B^+ center in **9** binds with each O in all three directions (p_x, p_y, and p_z), collectively leading to an extreme bonding situation that may be approximately described as $-O\equiv B^+\equiv O-$.

The hypervalent 3c–4e bond is a critical type of bonding beyond the Lewis structure concept.[2] An example is XeF_2, in which the p_x AOs of three atoms form a filled bonding CMO and a filled nonbonding CMO. The Xe center is believed to contribute two electrons to facilitate the formation of such an ω-bond. In structure **9**, the combination of HOMO − 5 and HOMO − 4 is analogous to the ω-bond in XeF_2, except that the former is a π bond in the p_y manifold, whereas the latter is a σ bond.[2] The same is true for the p_z manifold (HOMO − 5′ and HOMO − 4′). Dual 3c–4e bonds are nonexistent in XeF_2. It is stressed that the core B^+ center in **9** only possesses two valence electrons and hence each O center has to contribute 5 electrons, making the OBO bonding highly polar. Furthermore, the 3c–4e ω-bond in XeF_2 is effectively described as two F···Xe···F half bonds.[2] The same is true for the sixfold bonded B^+, where the dual 3c–4e ω-bonds may each be approximated as two half-bonds, resulting in low NRT bond orders in the OBO core (Table S7 in the ESI†). Similar OBO structural blocks and dual 3c–4e hypervalent bonds were very recently characterized in ternary and quaternary systems, such as the $LiB_2O_3^-$, $AuB_2O_3^-$, and $LiAuB_2O_3^-$ clusters and their neutral species.[27]

Interestingly, the core O atoms in **3**, **6**, and **9** all exhaust their 2s and 2p valence electrons (at least formally) in order to facilitate the formation of BO bonds, leading to O centers with fourfold bonds: $-B^+\equiv O-$. An example is shown for **3** in Fig. 2a and c. This bonding capability manages to compensate for the electron-deficiency of the system, which may hold the key to elucidating the bonding in the boron oxide systems.

4.4. Rhombic 4c–4e bonds (o-bonds)

A rhombic B_2O_2 unit is developed in **5**, **7**, and **8**, which appears to be structurally flexible with variable BO distances (Fig. 1). The rhombic B_2O_2 unit is dominated by the 4c–4e bond (Fig. 2e), which we prefer to call an ''o-bond''. Here HOMO − 7 is a delocalized, *bonding* π CMO composed of O $2p_z$ and B $2p_z$ AOs, whereas HOMO − 1 is essentially *nonbonding* due to O $2p_z$ AOs. This combination is closely analogous to the hypervalent 3c–4e ω-bond in **9** and in XeF_2. The o-bond may thus be viewed as an extension of the ω-bond, from three-center to four-center cases. It is stressed that a 4c–4e o-bond should not be confused with a 4π antiaromatic system. The 4c–4e o-bond is a *nonbonding*/*bonding* combination of two π orbitals, in contrast to an *antibonding*/*bonding* combination in a 4π antiaromatic system. The o-bond is thus essentially a 2π delocalized system due to the lack of an antibonding component, for which the 4*n* Hückel rule for antiaromaticity does not apply. The calculated nucleus independent chemical shift (NICS) values are negative: −2.04, −3.04, and −2.75 ppm at 1 Å above the center of the o-bond in **5**, **7**, and **8**, respectively. We note that a 4π antiaromatic system should be rectangular rather than rhombic.

To demonstrate the usefulness of the AdNDP method in bonding analyses for complex systems, we present the AdNDP results of $B_3O_4^-$ (**7**). As shown in Fig. 4, the 2c–2e terminal $B\equiv O$ and $B=O$ bonds, 2c–2e rhombic B–O bonds, and 2c–2e B–B single bonds are clearly revealed, as are the five O lone-pairs. The remaining (nonbonding) 2c–2e and (delocalized) 4c–2e bonds are responsible for the global bonding within the rhombic B_2O_2 unit, forming a typical 4c–4e o-bond. This analysis is reflected explicitly in Fig. 3g. The rhombic 4c–4e o-bond highlights the delocalization potency of O 2p AOs within the multicenter rings, which may be further developed to five-center and six-center units, the latter boroxol B_3O_3 ring being the dominant structural block in bulk boron oxide glasses and high-temperature liquids.[28,29] The boroxol ring may be considered a delocalized six-center six-electron (6c–6e) π system,[30] an extension of the 3c–4e ω-bond and the 4c–4e o-bond.

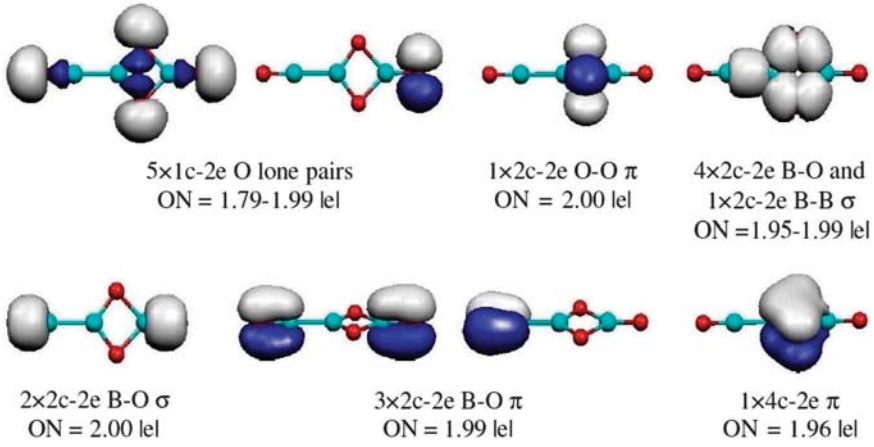

Fig. 4 AdNDP analysis of the bonding pattern in $B_3O_4^-$ (**7**), featuring its rhombic 4c–4e bond (o-bond).

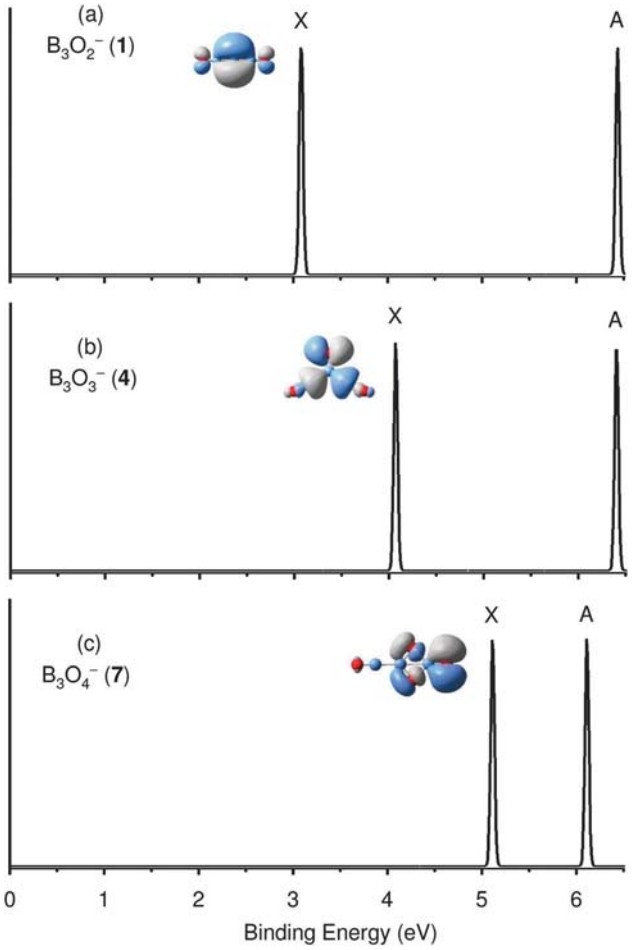

Fig. 5 Simulated photoelectron spectra of global-minimum anion structures **1**, **4**, and **7** on the basis of TD-B3LYP calculations. The simulations were done by fitting the distribution of the calculated VDEs with unit-area Gaussian functions of 0.05 eV half-width.

4.5. Simulated photoelectron spectra

To facilitate forthcoming experimental characterizations of the $B_3O_n^-$ and B_3O_n (n = 2–4) clusters, for example, using anion photoelectron spectroscopy (PES), we have calculated the ground-state vertical detachment energies (VDEs) of **1**, **4**, and **7** at the B3LYP level, calculated their higher VDEs for the excited-state transitions using TD-B3LYP, and simulated their PES spectra, as shown in Fig. 5. The numerical data are included in Table S8 in the ESI.† The ground-state VDEs of **1**, **4**, and **7** increase markedly and monotonically with the O content, by ~1 eV per O atom, demonstrating a process of sequential oxidation along the series. This VDE trend is also in line with the nature of the frontier CMOs of these species: The HOMO of **1** is a B 2p based bonding CMO, that of **4** has a certain O 2p lone-pair character with an antibonding mixture from B, whereas that of **7** is of primary O 2p character. As a consequence, the X–A energy gap reduces along the series. We also calculated the vertical ionization potentials for the neutral **2**, **5**, and **8** species, which amount to 9.81, 10.42, and 10.64 eV, respectively, at the B3LYP level.

It is noted that for the current $B_3O_n^{-/0/+}$ (**1–9**) clusters, since both photodetachment and photoionization are primarily one-electron processes, we generally cannot reach the neutral global minimum from an anion upon photodetachment, nor can we access the cation global minimum from a neutral species upon photoionization. It is therefore not very meaningful to calculate, for example, an "adiabatic" detachment energy from **4** to **5**, or an "adiabatic" ionization potential from **5** to **6**. The calculated adiabatic ionization energy minus adiabatic electron affinity of the **2**, **5**, and **8** neutral species does not correlate with the HOMO–LUMO gap, because the neutral species are not closed-shell.

5. Conclusions

In conclusion, we have studied the structural and electronic properties and chemical bonding in boron oxide clusters, *via* global-minimum searches and density-functional theory (B3LYP) and molecular orbital theory (CCSD(T)) calculations. Geometric structures of boron oxide clusters are shown to be size and charge-state dependent, thus every atom and electron counts. Unusual bonding features are uncovered for such an electron-deficient system: core boronyl groups, a terminal B site with lone-pair character, dual 3c–4e hypervalent ω-bonds, and rhombic 4c–4e σ-bonds. The potency of O centers to contribute and exhaust their 2s/2p valence electrons to form BO bonds help compensate for boron's electron-deficiency in the boron oxide systems. Furthermore, the rhombic 4c–4e σ-bond can be considered as the embryo form of the multicenter delocalized bonding, marking the genesis of the celebrated boroxol ring and aromaticity of boron oxide clusters, compounds, and materials.

Acknowledgements

This work was supported by the National Natural Science Foundation of China (No. 21243004 and 21373130). H.J.Z. gratefully acknowledges the start-up fund from Shanxi University for support.

References

1 W. N. Lipscomb, *Boron Hydrides*, W. A. Benjamin, New York, 1963.
2 F. Weinhold and C. R. Landis, *Valency and Bonding: A Natural Bond Orbital Donor-Acceptor Perspective*, Cambridge University Press, Cambridge, 2005, pp. 275–351.
3 I. Boustani, *Phys. Rev. B: Condens. Matter Mater. Phys.*, 1997, **55**, 16426.
4 J. E. Fowler and J. M. Ugalde, *J. Phys. Chem. A*, 2000, **104**, 397.
5 J. I. Aihara, H. Kanno and T. Ishida, *J. Am. Chem. Soc.*, 2005, **127**, 13324.
6 A. N. Alexandrova, A. I. Boldyrev, H. J. Zhai and L. S. Wang, *Coord. Chem. Rev.*, 2006, **250**, 2811.
7 (*a*) H. J. Zhai, A. N. Alexandrova, K. A. Birch, A. I. Boldyrev and L. S. Wang, *Angew. Chem., Int. Ed.*, 2003, **42**, 6004;

(*b*) H. J. Zhai, B. Kiran, J. Li and L. S. Wang, *Nat. Mater.*, 2003, **2**, 827.

8 (*a*) A. N. Alexandrova, A. I. Boldyrev, H. J. Zhai, L. S. Wang, E. Steiner and P. W. Fowler, *J. Phys. Chem. A*, 2003, **107**, 1359; (*b*) A. P. Sergeeva, D. Yu. Zubarev, H. J. Zhai, A. I. Boldyrev and L. S. Wang, *J. Am. Chem. Soc.*, 2008, **130**, 7244; (*c*) W. Huang, A. P. Sergeeva, H. J. Zhai, B. B. Averkiev, L. S. Wang and A. I. Boldyrev, *Nat. Chem.*, 2010, **2**, 202; (*d*) A. P. Sergeeva, Z. A. Piazza, C. Romanescu, W. L. Li, A. I. Boldyrev and L. S. Wang, *J. Am. Chem. Soc.*, 2012, **134**, 18065.

9 M. L. Drummond, V. Meunier and B. G. Sumpter, *J. Phys. Chem. A*, 2007, **111**, 6539.

10 (*a*) T. B. Tai and M. T. Nguyen, *Chem. Phys. Lett.*, 2009, **483**, 35; (*b*) M. T. Nguyen, M. H. Matus, V. T. Ngan, D. J. Grant and D. A. Dixon, *J. Phys. Chem. A*, 2009, **113**, 4895; (*c*) T. B. Tai, M. T. Nguyen and D. A. Dixon, *J. Phys. Chem. A*, 2010, **114**, 2893.

11 R. J. Doyle, *J. Am. Chem. Soc.*, 1988, **110**, 4120.

12 H. Braunschweig, K. Radacki and A. Schneider, *Science*, 2010, **328**, 345.

13 H. J. Zhai, S. D. Li and L. S. Wang, *J. Am. Chem. Soc.*, 2007, **129**, 9254.

14 S. D. Li, H. J. Zhai and L. S. Wang, *J. Am. Chem. Soc.*, 2008, **130**, 2573.

15 (*a*) H. J. Zhai, J. C. Guo, S. D. Li and L. S. Wang, *ChemPhysChem*, 2011, **12**, 2549; (*b*) J. C. Guo, H. G. Lu, H. J. Zhai and S. D. Li, *J. Phys. Chem. A*, 2013, **117**, 11587.

16 A. P. Sergeeva, B. B. Averkiev, H. J. Zhai, A. I. Boldyrev and L. S. Wang, *J. Chem. Phys.*, 2011, **134**, 224304.

17 (*a*) M. Saunders, *J. Comput. Chem.*, 2004, **25**, 621; (*b*) P. P. Bera, K. W. Sattelmeyer, M. Saunders and P. v. R. Schleyer, *J. Phys. Chem. A*, 2006, **110**, 4287.

18 H. Bai, Q. Chen, Y. F. Zhao, Y. B. Wu, H. G. Lu, J. Li and S. D. Li, *J. Mol. Model.*, 2013, **19**, 1195.

19 R. J. Bartlett and M. Musial, *Rev. Mod. Phys.*, 2007, **79**, 291.

20 E. D. Glendening, J. K. Badenhoop, A. E. Reed, J. E. Carpenter, J. A. Bohmann, C. M. Morales and F. Weinhold, *NBO 5.0.*, Theoretical Chemistry Institute, University of Wisconsin, Madison, 2001.

21 (*a*) M. E. Casida, C. Jamorski, K. C. Casida and D. R. Salahub, *J. Chem. Phys.*, 1998, **108**, 4439; (*b*) R. Bauernschmitt and R. Ahlrichs, *Chem. Phys. Lett.*, 1996, **256**, 454.

22 M. J. Frisch, *et al.*, *GAUSSIAN 09, revision A.2*, Gaussian, Inc., Wallingford, CT, 2009 (see the ESI†).

23 (*a*) A. Moezzi, M. M. Olmstead and P. P. Power, *J. Am. Chem. Soc.*, 1992, **114**, 2715; (*b*) A. Moezzi, R. A. Bartlett and P. P. Power, *Angew. Chem., Int. Ed. Engl.*, 1992, **31**, 1082.

24 D. Yu. Zubarev and A. I. Boldyrev, *Phys. Chem. Chem. Phys.*, 2008, **10**, 5207.

25 Quantitative bonding analysis using the electron localization function (ELF) does not appear to work well for the current system, due to the polar nature of the B–O bonding. For example, while boronyl (BO) is established in either gas-phase clusters or synthetic compounds as a genuine B$\equiv$O triple bond,[9–15] analogous to C$\equiv$O or C$\equiv$N, the ELF data suggest that among the 10 valence electrons in BO^-, $\sim$2.3 are located on B, $\sim$4.3 are located on O, and only $\sim$3.3 are populated in between. In contrast, ELF can correctly reproduce the bond orders of CC ($\sim$2.8 electrons) and CH ($\sim$2.1 electrons) in benzene, a typical covalent system. Thus, ELF clearly has its intrinsic limitation for the polar bonds, such as in the boron oxide system.

26 P. Pyykkö and M. Atsumi, *Chem.–Eur. J.*, 2009, **15**, 12770.

27 W. J. Tian, H. G. Xu, X. Y. Kong, Q. Chen, W. J. Zheng, H. J. Zhai and S. D. Li, *Phys. Chem. Chem. Phys.*, 2014, **16**, 5129.

28 G. Ferlat, T. Charpentier, A. P. Seitsonen, A. Takada, M. Lazzeri, L. Cormier, G. Calas and F. Mauri, *Phys. Rev. Lett.*, 2008, **101**, 065504.

29 J. D. Mackenzie, *J. Phys. Chem.*, 1959, **63**, 1875.

30 D. Z. Li, H. Bai, Q. Chen, H. G. Lu, H. J. Zhai and S. D. Li, *J. Chem. Phys.*, 2013, **138**, 244304.